Structure, Vol. 10, 921–931, July, 2002, ©2002 Elsevier Science Ltd. All rights reserved. PII S0969-2126(02)00789-X

A Dynamic Analysis of the Rotation Mechanism for Conformational Change in F_1-ATPase

Jianpeng Ma,[1,2,3] Terence C. Flynn,[1,2] Qiang Cui,[3,4] Andrew G.W. Leslie,[5] John E. Walker,[6] and Martin Karplus[3,7,8]

[1]Department of Biochemistry and Molecular Biology
Baylor College of Medicine
One Baylor Plaza, BCM-125
Houston, Texas 77030

[2]Department of Bioengineering
Rice University
6100 Main, MS-142
Houston, Texas 77005

[3]Department of Chemistry and Chemical Biology
Harvard University
12 Oxford Street
Cambridge, Massachusetts 02138

[4]Department of Chemistry
University of Wisconsin, Madison
1101 University Avenue
Madison, Wisconsin 53706

[5]Medical Research Council Laboratory of Molecular Biology
Hills Road
Cambridge CB2 2QH
United Kingdom

[6]Medical Research Council Dunn Human Nutrition Unit
Hills Road
Cambridge CB2 2XY
United Kingdom

[7]Laboratoire de Chimie Biophysique, ISIS
Université Louis Pasteur
67000 Strasbourg
France

Summary

Molecular dynamics trajectories for the bovine mitochondrial F_1-ATPase are used to demonstrate the motions and interactions that take place during the elementary (120° rotation) step of the γ subunit. The results show how rotation of the γ subunit induces the observed structural changes in the catalytic β subunits. Both steric and electrostatic interactions contribute. An "ionic track" of Arg and Lys residues on the protruding portion of the γ subunit plays a role in guiding the motions of the β subunits. Experimental data for mutants of the DELSEED motif and the hinge region are interpreted on the basis of the molecular dynamics results. The trajectory provides a unified dynamic description of the coupled subunit motions involved in the 120° rotation cycles of F_1-ATPase.

Introduction

The enzyme F_1F_o-ATP synthase, found in eubacteria, chloroplasts, and mitochondria, is responsible for most of the ATP synthesis in living systems [1–3]. It is a large multisubunit complex consisting of a proton-translocating membrane domain, F_o, attached via central and peripheral stalks to the catalytic domain F_1, a spherical globular structure outside the membrane. The F_1 domain, F_1-ATPase, is made of three α and three β subunits arranged in alternation around a central α-helical coiled-coil structure that is a continuation of the central stalk [4]. The foot of the central stalk makes extensive contacts with a ring [5] of c subunits in the membrane domain [5]. In yeast mitochondria ten c subunits form the ring, and there is evidence for stoichiometries in the range from 10 to 14 in other species [6–8]. The central stalk and the associated c ring are believed to rotate as an ensemble relative to the rest of the enzyme, the rotation being generated by the transmembrane protonmotive force via photosynthesis or respiration. The central stalk consists of the γ subunit with the associated δ and ϵ subunits. The α-helical coiled-coil domain of the γ subunit is asymmetric, and the rotation of this asymmetrical structure appears to modulate the binding affinities of the catalytic β subunits for substrate and products. Each of them, in turn, goes through three states known as "open" (or empty), "loose," and "tight", in accord with the "binding change" mechanism of ATP synthesis [9–10]. The open subunit (which corresponds to β_E in the X-ray structure of Abrahams et al. [4]) has a low affinity for either substrate or product. According to this mechanism, during the synthesis cycle of F_1F_o-ATP synthase, a rotation of 120° converts an open site, with low affinity for substrate or product, into a loose substrate binding state. A further 120° rotation converts the loose state to the tight state, and the product ATP is formed. Another 120° rotation converts the tight state back to the open state, releasing the ATP product. In the X-ray structure of Abrahams et al. [4], the β_E subunit (no bound nucleotide) was identified as representing the open state, the β_{TP} subunit (AMP-PNP bound) was identified as representing the loose state, and the β_{DP} subunit (ADP bound) was identified as representing the tight state. A more detailed discussion of a suggested assignment of the observed conformations of the β subunits to the different states of the binding change mechanism is given in Menz et al. [11].

The F_1 domain can be separated from the membrane domain, and it retains the ability to hydrolyze ATP. Hydrolysis of ATP leads to the rotation of the central stalk, though the detailed mechanism is not understood. By attaching an actin filament or a bead to the exposed foot of the central stalk, the rotation has been visualized in a microscope [12]. It turns counterclockwise (as viewed from the membrane) in 120° steps. During the ATP synthesis cycle, which we study here, the rotation of the central stalk is presumed to be in the opposite sense.

Comparisons of the subunits within a given structure and in different structures have provided important clues

[8]Correspondence: marci@tammy.harvard.edu

Key words: F_1-ATPase; molecular dynamics simulation; ATP synthesis; molecular motors; rotatary catalysis; targeted molecular dynamics

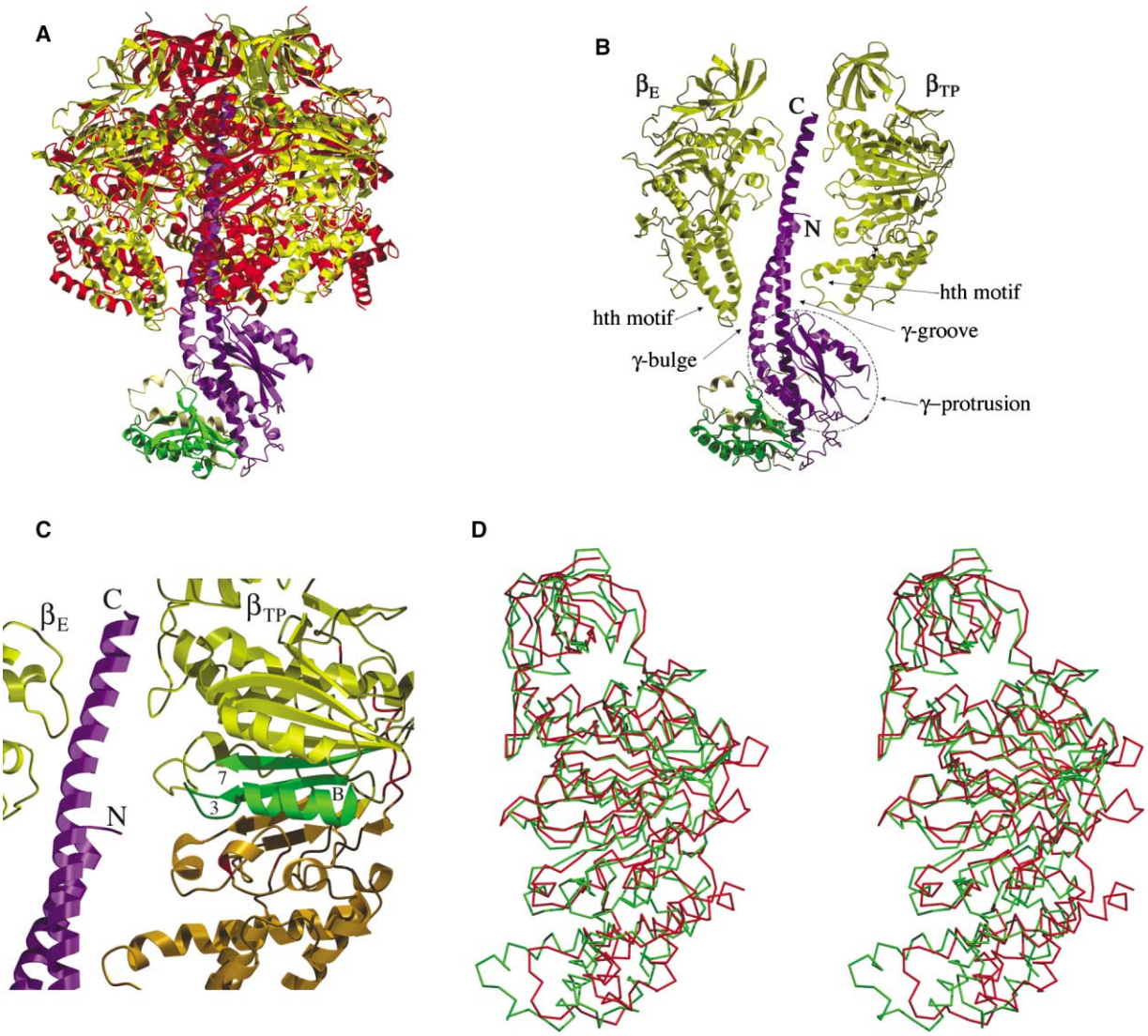

Figure 1. Views of the F_1-ATPase Structure

(A) Ribbon structure of F_1-ATP synthase showing $\alpha_3\beta_3\gamma\delta\epsilon$ based on the structures of Abrahams et al. [4] and Gibbons et al. [15] (see Experimental Procedures). α subunits, red; β subunits, yellow; γ subunit, purple; δ subunit, green; ϵ subunit, light yellow.

(B) View showing β_E and β_{TP}, plus γ, ϵ, and δ, from same structures as in (A) with labels, including γ bulge, γ groove, and γ protrusion.

(C) Detail from Figure 1B showing central portion of β_{TP} subunit with coiled coil of γ subunit (purple) and illustrating some important structural elements mentioned in the text. The central domain is shown in yellow, with the β strands 3 and 7 and helix B highlighted in green and the hinge region plus the flexible loop made up of residues 119–134 in red. A portion of the C-terminal domain is shown in gold, with the Phe418 and 424 loop region in red.

(D) Stereo view showing α_{TP} in red and β_{TP} in green, with the N-terminal domain and the top of the central domain superposed. See text for subunit labels.

concerning the rotational mechanism of F_1-ATPase. However, a direct study of the transition at an atomic level of detail is essential for determining the dynamics of the structural changes and the relative order in which they occur. The analysis reported here, which is based primarily on simulations with the targeted molecular dynamics (TMD) method [13], is an important step toward this goal. We supplement the TMD results with those based on the biased molecular dynamics (BMD) method [14]. The structural model we use for the simulation was obtained (see Experimental Procedures) by combining the original X-ray structure of F_1-ATPase [4] with a more recent structure that has resolved most of the γ, δ, and ϵ subunits [15]. The simulations correspond to a single 120° rotation step in the direction of ATP synthesis, with the γ subunit rotating in a clockwise direction, as viewed from the bottom of Figure 1A. The α and β subunits do not rotate but undergo conformational changes based on the endstates inferred from the X-ray structure of Abrahams et al. [4]. As described in Experimental Procedures, the TMD simulation applies constraints to the entire system to find a low energy pathway connecting the two endstates. By constrast, in the BMD simulation (see Experimental Procedures), a biasing force is ap-

plied only to the γ subunit to determine directly the response of the α and β subunits to the rotation of the γ subunit; it provides some important supplementary results, as described below, but it does not yield the full transition path obtained with the TMD method over the nanosecond timescale of the trajectory.

The trajectory has the spatial and temporal resolution necessary to reveal the structural and energetic origins of the conformational changes that occur during the 120° rotation step. Specifically, the results demonstrate how the rotation of the γ subunit induces the major changes observed in the structure of the β subunits. The lower part of the γ subunit, including the $\alpha\beta$ domain, which protrudes from the $\alpha_3\beta_3$ complex (it is referred to as the "γ protrusion" below), is shown to play an essential role in the dynamics of the transition. Some α subunit motions occur during the transition, although all three are very similar in the X-ray structure. Certain side chain interactions, such as those involving the ionic track of the γ subunit, are shown to be important in guiding the transition. The closing motion of the β_E subunit, with ADP bound, involves primarily electrostatic interactions, while the outward movement of the β_{TP} subunit, with no ligand, is due primarily to steric interactions with the γ subunit. Main chain polar interactions of the DELSEED motif supplement those from the negatively charged side chains and explain the fact that mutation of the latter does not inactivate the rotational mechanism. A more detailed description of the motion in the hinge region than that inferred from the X-ray structure is obtained. The molecular dynamics trajectory reported here provides a unified description of the subunit motions of F_1-ATPase in the 120° rotation cycle that forms the basis for its function.

Results

Coupled Subunit Motions in the 120° Synthesis Step

Overall Structure

The overall structure of the bovine mitochondrial F_1-ATPase is available from Abrahams et al. ([4]; see Figure 1A). It consists of nine subunits referred to as $\alpha_3\beta_3\gamma\delta\epsilon$, has an approximately spherical domain about 100 Å across and 80 Å high, with a stalk that protrudes by about 45 Å, and interacts with the membrane-bound F_o portion of the F_1F_o-ATP synthase complex. The three α and three β subunits that form the spherical domain are associated with each other like the segments of an orange. The γ subunit consists of a left-handed α-helical coiled coil formed by a shorter N-terminal helix and a longer C-terminal helix, which occupy a central hole in the $\alpha_3\beta_3$ complex, and a more globular portion that forms the γ protrusion, which includes the lower part of the coiled coil. The δ and ϵ subunits are associated with the γ protrusion but are not in contact with the $\alpha_3\beta_3$ portion of the complex and do not play an important role in the rotation studied here, though they are likely to be involved in coupling to the F_o complex. The α and β subunits have similar folds, and each one can be divided into an N-terminal β barrel domain, a central nucleotide binding domain, and a C-terminal helical domain. The N-terminal domains of the six subunits form a ring with roughly 6-fold symmetry that is believed to play a major role in the stability of the $\alpha_3\beta_3$ complex and undergoes small changes during the transition. The conformations of the central domains and the C-terminal domains of β_{TP} and β_{DP}, which have AMP-PNP and ADP bound, respectively, are very similar to each other (for notation, see Figure 1B and its legend). The empty β_E subunit has a very different conformation, although the overall fold is similar to that of the other subunits. The nucleotide binding site in the central domain of β_E is open, when compared with β_{TP}, due to a conformational change. It involves the separation of the C-terminal portions of β strands 7 and 3, movement (and increased disorder) of the loop containing Phe418 and Phe424, and a global increase in the distance between the α and β subunits in the vicinity of the binding site, as described and illustrated in Abrahams et al. [4]; we focus here on the separation of β strands 7 and 3 as a marker for the nucleotide binding site opening in what follows (see Figure 1C). In β_E, there is also a displacement of helix B of the central domain and a large downward rotation of the C-terminal domain when compared with the corresponding domains of β_{TP} and β_{DP}. The three α subunits, which bind AMP-PNP, have a closed nucleotide binding site and N-terminal and central domains that are very similar to those of β_{TP} and β_{DP}. However, the C-terminal domains of the α subunits are significantly different from those of β_{TP} and β_{DP} (Figure 1D); this is found to be important in the rotational motion. The γ subunit is positioned such that its "bulge," formed by the N-terminal helix above the protrusion, faces the C-terminal domain of the empty β_E subunit and its "groove," formed by the other side of the N-terminal and C-terminal coiled-coil helices, faces the C-terminal domains of the β_{DP} and β_{TP} subunits (Figure 1B). The helix-turn-helix (hth) motifs (Figure 1B) of the β subunit C-terminal domains play an essential role in the interaction with the γ subunit. In the crystal structure, those of β_{DP} and β_{TP} are in van der Waals contact with each other within the γ groove, while that of the β_E subunit is pushed outward by the γ bulge.

γ *Subunit Motion*

Since the conformational changes of the β subunits in the ATP synthesis cycle are "driven" by the γ subunit, we first describe its motions. We use the fractional time (in percent) along the trajectory to order the events that occur during the transition. The calculation time (between 250 ps and 1 ns) is much shorter than the actual timescale (on the order of 250 μs for a 120° rotation in hydrolysis [16]), but the correspondence of the results obtained with simulations of different lengths (see Experimental Procedures) provides support for identifying the dynamics that take place during the trajectory with the physical motions. The rotation of the γ protrusion is rather uniform up to about 90° (60% of the trajectory); the remainder of the rotation occurs more slowly and is essentially complete at 90% of the trajectory, with only small adjustments after that. There is little "trembling" of the axis during the transition, indicating that the description of the γ subunit motion as a rotation is meaningful. Although the motions of the portions of the N- and C-terminal helices within the γ protrusion are essentially synchronized with it, the rotation of the coiled-coil por-

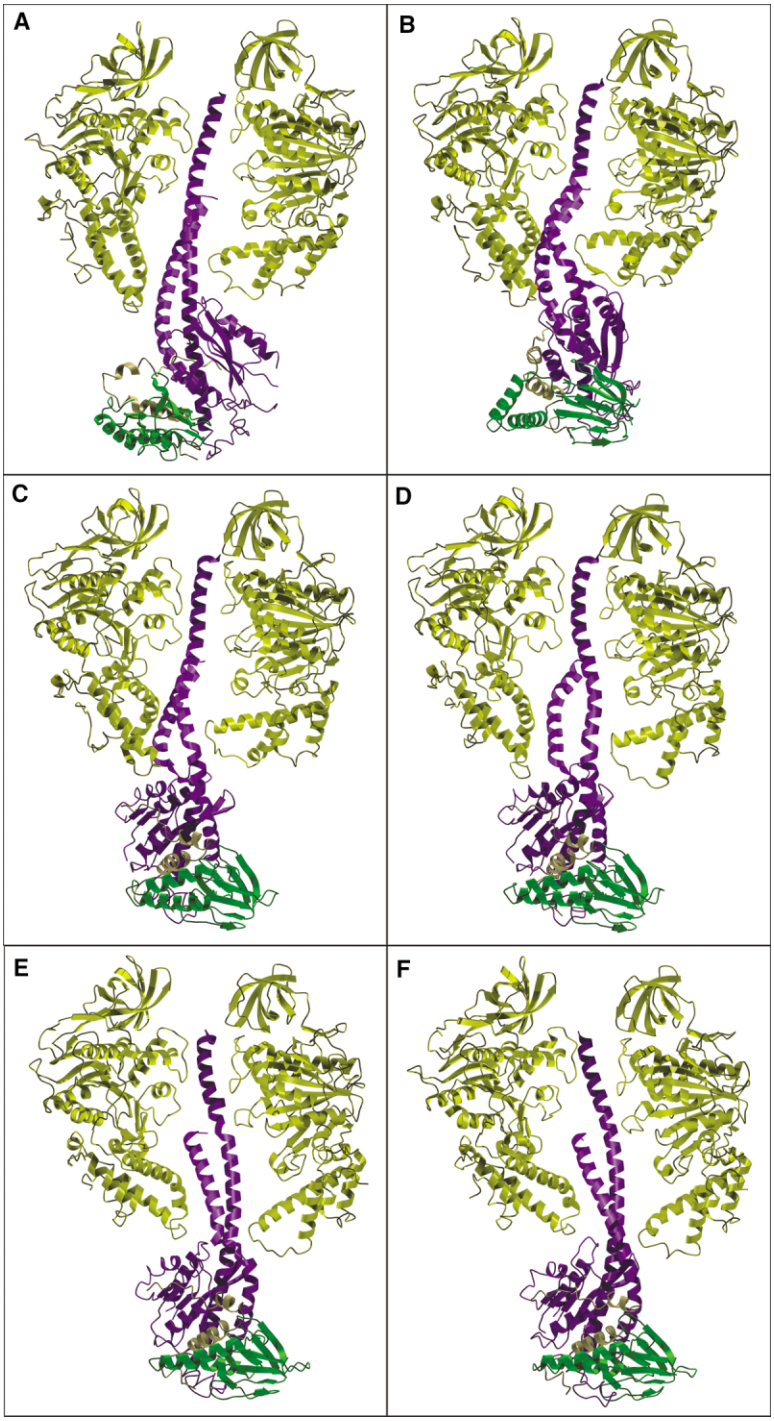

Figure 2. Structures from the Molecular Dynamics Trajectory Showing β_E, β_{TP}, γ, δ, and ϵ in Same Colors as in Figure 1A

Intitial structure (A); 150 ps (B); 300 ps (C); 350 ps (D); 425 ps (E); final structure (F).

tion that extends above the γ protrusion lags behind somewhat. It has rotated by about 80° at 80% of the trajectory, and the top part of the C-terminal helix completes its rotation at the end of the trajectory. The γ subunit rotation, as well as the conformational change of β_{TP} and β_E during the trajectory, are visualized in Figure 2. During ATP synthesis, the rotation of the γ subunit is driven by the translocation of protons through the transmembrane segment, F_o. The observed lag and the distortion of the coiled coil reflects the energetic barriers that must be overcome in inducing the conformation change of the β subunits during the synthesis cycle. That the coiled coil is flexible has been suggested from a comparison of X-ray structures [11]. A normal mode analysis indicates that the lowest modes of the γ subunit involve a twisting/untwisting of the coiled coil, with the γ protrusion undergoing a small rocking motion (data not shown).

$\alpha_3\beta_3$ *Subunit Motions*

At the start of the trajectory (see Figure 2), the γ bulge of the N-terminal helix is oriented directly toward β_E; after the 120° rotation, the γ bulge is oriented toward

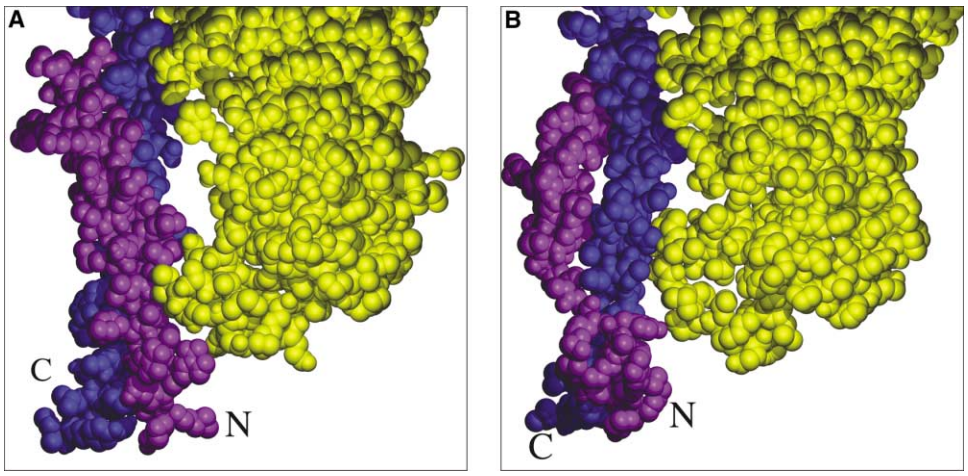

Figure 3. Space-Filling View of Parts of β_{TP} in Yellow and the Coiled Coil of the γ Subunit, with the N-Terminal Helix and Its γ Bulge in Magenta and the C-Terminal Helix and its γ Bend in Dark Purple

(A) Intermediate structure corresponding to Figure 2D showing the hth motif of β_{TP} being "pushed out" by the γ bend of the C-terminal helix.
(B) Final structure showing β_{TP} in contact with the γ bulge of the N-terminal helix; see text.

β_{TP}. The downward and outward displacement of the hth motif of β_{TP}, which is located in the γ groove at the beginning of the trajectory, is initiated by the steric repulsion between the hth motif and the "γ bend" (i.e., the curved C-terminal helix of the γ subunit) in the middle of the trajectory (50%), when the γ protrusion has rotated by about 70°, and is completed near the end of the rotation cycle (90%), when the hth motif is in contact with the γ bulge (Figure 3). Throughout the transition, the hth motif is guided by its interactions with the ionic track (see below). The motion of the hth motif leads to the displacement of the entire C-terminal domain of β_{TP} and is coupled to the conformational change in the central domain; e.g., the breaking of the hydrogen bonds between β strands 7 and 3, which opens the nucleotide binding site. The lower portion of the central domain and the C-terminal domain move approximately as a unit, although there are also significant internal motions during the transition. As pointed out by Masaike et al. [17], the largest main chain dihedral angle changes involve three "hinge" residues, His177, Gly178, and Gly179. However, there are many smaller changes in the region around the hinge, indicating that the opening transition is more like a relatively localized elastic body motion. Examples are the deformation of the B helix during the dynamics, which results in an extra turn in β_E relative to β_{TP}, and the rearrangements in a loop (residues 119–134) connecting the two parts of the central domain; the structures sampled during the dynamics involve motions not evident from an interpolation between the end structures. The result of Masaike et al. [17], that mutating two hinge residues, Gly178 and Gly179, to Ala had only a small effect on the hydrolysis reaction, indicates the complexity of the motion. Only when His177 was also mutated to Ala was essentially complete inhibition achieved. The latter mutation is not likely to contribute sterically to preventing the conformation change. As can be seen from the crystal structure, His177 in the closed state (β_{TP}) forms a strong hydrogen bond with the main chain carbonyl of Tyr180 and a weaker one with Asp250. During the dynamics, His177 moves outward, and it points away from these residues in the open state. Since Tyr180 is at the other end of the turn formed by residues 177–180, the His177, Tyr180 interaction is expected to play a significant role in stabilizing the closed form.

The inward motion of β_E induced by the γ subunit rotation is somewhat more complex than the outward motion of β_{TP} just described. The initial position of β_E is constrained by the steric (van der Waals) interactions between its hth motif and the γ bulge. As the γ subunit rotates and the γ bulge passes by the hth motif (near 40%), the latter is distorted by it. The hth motif then assumes a less distorted structure and starts to be pulled into the γ groove, mainly by electrostatic interactions (see below). This causes an upward motion of the rest of the C-terminal domain and leads to the closing of the nucleotide binding site with restructuring of the β sheet by hydrogen bond formation between strands 3 and 7 in the central domain; this occurs slightly later (60%). As was found for β_{TP}, the relative motions of β_E and the γ subunit are guided by the ionic track on the protrusion of the latter (see below). The motion of β_E involves both repulsive and attractive interactions with the coiled coil of the γ subunit; i.e., steric repulsion with the γ subunit first prevents entrance into the groove, but, once the γ bulge has passed, attractive ionic interactions pull the hth motif inward in the simulation. This occurs spontaneously, as shown by the BMD simulation (see below). By the choice of the occupation of the β subunit nucleotide binding sites, in accord with the endstate (i.e., that which occurs after the 120° rotation), the contributions of the ligands to the conformation change are included implicitly, i.e., the empty β_{TP}-site opens, while the ADP-containing β_E-site is induced to close.

Previously, it has not been possible to infer anything concerning the motions of the α subunits because they are very similar in the crystal structures (e.g., Abrahams et al. [4]). They remain in the closed form, in accord with

the experimental observation that the α subunits do not exchange ATP or its analogs on the timescale of catalysis [1]. A major reason for the small motion of the α subunits is that their tertiary structure is different from those of β_{TP} and β_{DP} (see Figure 1D). Although the N-terminal and much of the central domains of the α and β subunit are essentially superposable in the X-ray structure, the C-terminal domain of the α subunits is oriented such that its hth motif is further away from the γ subunit than are the hth motifs of β_{TP} and β_{DP}. This is due, in part, to the fact that helix 1 of the hth motif in the α subunits is shorter than the corresponding helix in the β subunits. Thus, as shown in the simulation, the γ bulge can pass without a major collision with the α subunits. Nevertheless, the α subunits do undergo transient distortions. The α_{DP} subunit has some distortion of the hth motif during the transition, first due to repulsions from the γ protrusion and then at about 80% completion due to interactions with the C-terminal helix of the γ subunit, which ends up in contact with the hth motif. α_{TP} initially interacts with the C-terminal helix of the γ subunit; at about 80%, the C-terminal helix has moved past, and the hth motif assumes its undistorted form, which is again disturbed slightly as the γ bulge passes by. α_E interacts with neither of the coiled-coil helices of the γ subunit; instead, the hth motif collides with the γ protrusion during the rotation and is pushed slightly upward by it.

The interactions (steric and electrostatic) of the rotating γ subunit with the $\alpha_3\beta_3$ complex provide the major driving force in the synthase cycle; nevertheless, it is also of interest to examine the interactions among the α and β subunits. The only significant contact between identical subunits is that between β_{TP} and β_{DP} in the initial state and that between β_{DP} and β_E in the final state. When the hth motif of the β_E subunit moves inward, it establishes a stabilizing van der Waals contact with the hth motif of the β_{DP} subunit and, at the same time, the corresponding contacts between β_{TP} and β_{DP} are broken; the calculated interaction energy between the two subunits in contact is about 3 kcal/mol. During this process, the β_{DP} subunit undergoes only a small structural change. There are no contacts between any pair of α subunits during the transition, including the endpoint structures. However, there are significant interactions between individual α and β subunits, and the α subunits contribute to forming the β subunit active sites [4]. From the simulation, the α subunits are important not only for the structural integrity of the F_1 complex (they act as spacers between the β subunits) but also for positioning of the β subunits, such that they undergo the required conformational changes in response to the rotation of the γ subunit. The contacts between the various α and β subunits differ somewhat. α_{DP} and β_{DP} are in close van der Waals contact, with α_{DP} quite far from the γ subunit, and both α_{DP} and β_{DP} move very little during the transition. The contacts between the β_{TP} and α_{TP} subunits are less extensive, while the β_E and α_E subunits are in contact only through the N-terminal domains and the upper region of the nucleotide binding domains.

The Interactions Contributing to the Rotational Transition

Although the major structural changes during the ATP synthase cycle can be described by reference to the main chains, the interactions between the subunits that produce these changes arise primarily from the side chains, although the main chain also contributes. The large conformation changes of the β_E and β_{TP} subunits during the rotation cycle are initiated by interactions of their hth motifs with the central γ subunit, although other parts of the β subunits are also involved. The major contributions come from steric repulsions due to van der Waals terms and electrostatic attractions between the side chains and the main chain of certain residues; van der Waals attractions play a smaller role. Figure 4 shows a space-filling model to illustrate the steric interactions between the γ bulge and γ bend and the hth motifs of the β subunits.

A striking observation from the calculated rotational transition concerns the electrostatic interactions between the γ and β subunits (Figures 4 and 5). They are found to mediate the coupled motion of the γ subunit and the three β subunits, as presaged in the "catch" residues proposed by Abrahams et al. [4]. The γ subunit has a large number of positive side chains (16 Arg and 22 Lys), which are distributed in two distinct regions. Most of them are on the upper surface of the γ protrusion, including the lower part of the coiled coil, and the others are on the upper parts of the coiled coil. Figures 4A and 4B show the distribution of the positively charged side chains on the γ protrusion. These positive side chains form an ionic track that interacts with negatively charged side chains (Glu and Asp) located on the β subunits. A schematic "road map" of the interactions that occur during the 120° rotation between the ionic track and the negatively charged side chains of the hth motif is given in Figure 5. The figure is drawn as viewed from the top and shows that the positive amino acids form an essentially continuous "track" around the upper surface of the γ protrusion. As the γ subunit rotates, the negative side chains on the hth motif of the β subunits make sequential ionic contacts with some of the positive side chains along the track. For example, Asp394 and Glu395 of the DELSEED loop in the hth motif of the β_E subunit, which are initially in contact with Arg36 of the γ subunit, step along the ionic track and, after moving nearly 38 Å during the 120° rotation, engage with Arg228 and Lys11 in the γ groove. Asp394 and Glu395 sequentially contact Arg33, Lys30, and Arg134 along the track. Correspondingly, Asp394, Glu395, and Glu398 in the hth motif of the β_{TP} subunit, which are in contact with Lys87 and Lys90 of the γ protrusion at the beginning (the "second catch" noted by Abrahams et al. [4]), step along the other side of the track (containing Lys172, Arg166, Arg164, Arg42, and Lys39) and finally engage with Arg36. Asp394 and Glu395 of the β_{DP} subunit start in contact with Arg75, Arg133, and Arg228 in the γ groove and end up interacting with Lys87 and Lys90. The essentially continuous electrostatic track on the γ protrusion (Figure 5) provides a low-energy pathway for the negatively charged hth motifs of the β subunits, which "glide" smoothly from their initial to their final positions. In addition to the ionic track side chain-side chain interactions, other electrostatic interactions and some nonpolar contacts also play a role. For example, main chain carbonyls in the residues (Ala389–Gly392) adjacent to the DELSEED motif were found to interact strongly with Arg33 and Arg36 of the γ protrusion in the early stages

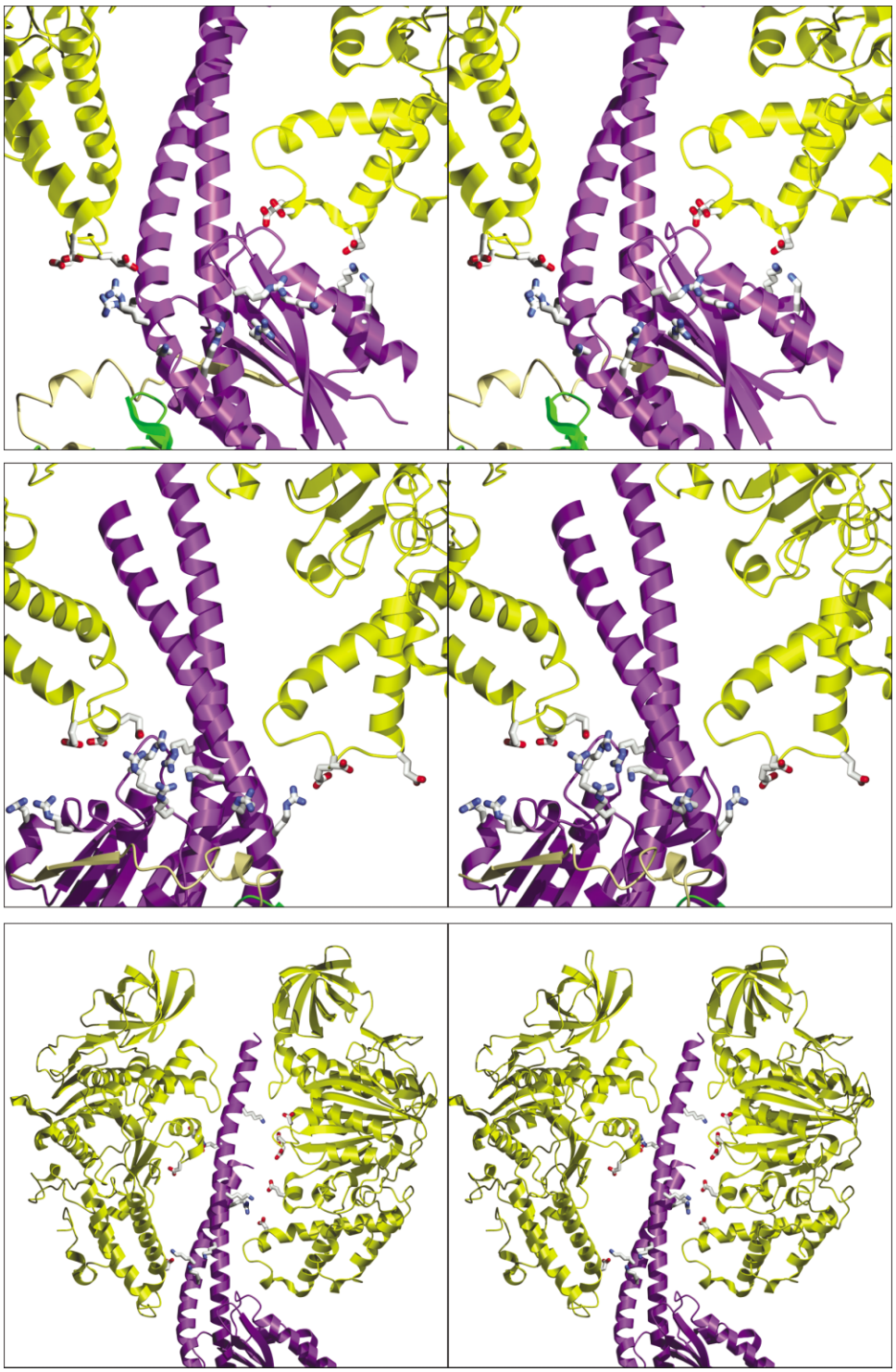

Figure 4. Stereoviews Showing Ionic Interactions between γ Subunit in Magenta and β Subunits in Yellow

(A) Initial structure showing β_E and β_{TP} with negatively charged side chains on their hth motifs and positively charged side chains on the γ protrusion in stick form.

(B) Initial structure showing β_{DP}, β_E, and the γ protrusion with charged side chains, rotated by about 120° with respect to (A) to show side chains on the other side of the γ protrusion.

(C) Positively charged side chains on γ coiled coil interacting with negatively charged side chains on β_E and β_{TP}.

of the simulation, then with Lys30, and finally with Arg75, Lys129, and Arg133. The contribution from main chain atoms is consistent with mutation experiments [18], which showed that the rotation induced by hydrolysis was only slightly affected when all five charged residues in the highly conserved DELSEED motif were mutated

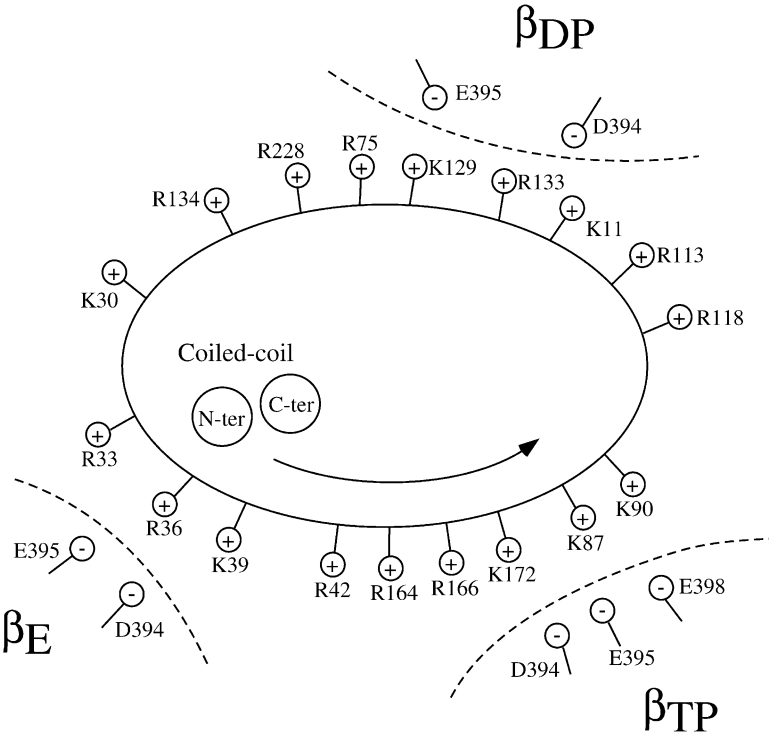

Figure 5. Schematic View of the Ionic Track Corresponding to Figures 4A and 4B

to alanine, although the catalytic activity was reduced by 30%. The role of the electrostatic interactions in closing motion of β_E was confirmed by a BMD simulation, in which the β subunits were subjected to no constraints (see Experimental Procedures). It was found in the BMD simulations that the β_E subunit with ADP bound moves spontaneously into its γ groove position, accompanied by reformation of the hydrogen bonds between strands 3 and 7 of the β sheet and closing of the binding site. This also indicates that the "intrinsic" timescale of the closing of the β_E subunit with bound ADP is in nanoseconds, although the motion is expected to occur more slowly during the actual rotation cycle, since it is controlled by the rotation of the γ subunit, which is on a submillisecond timescale. By contrast, the β_{TP} subunit in the BMD simulation was distorted after the 120° rotation of the γ subunit, as a result of repulsive interactions with the latter, but it did not reach the crystallographic end structure. Whether this is an artifact of the simulation or whether it indicates that slower motions are involved requires further studies. It does make clear, however, the importance of the TMD simulations for determining the complete path between the crystallographic endstates on the timescale accessible to the simulation.

Figure 4C shows a side view of the distribution of the electrostatic interactions along the coiled coil of the γ subunit. There are two main regions of the β_E and β_{TP} subunits that have electrostatic contacts with the central coiled coil. One involves the hth motif (lower region in Figure 4C) already discussed, and the other is a loop (residues Tyr311–Asp319) near the nucleotide binding site (middle region in Figure 4C; see also Abrahams et al. [4]; it is the loop between strand 7 and helix 6 in their Figure 2D). The corresponding negative side chains on the β_{DP} subunit make electrostatic contacts with the coiled coil exclusively near the tip of the N-terminal helix (e.g., Thr2 and Lys4). A cyclic swapping sequence, similar to that involving the ionic track on the γ protrusion, takes place when the γ subunit rotates. The DELSEED region of the β_E subunit form new interactions with the region around Ser 22 of the γ subunit as the latter rotates; as a result, the stabilizing interaction energy between the two subunits increases substantially in the second half of the rotation. This causes the hth motif of the β_E subunit to move upward toward the closed conformation. The resulting conformation is further stabilized in the final stage of the γ rotation by the interaction between Arg70 of β_E and the main chain of Gly71 of the γ subunit. Throughout the rotation, the central domain of the β_E subunit interacts strongly with the γ coiled coil by electrostatic terms between Asp315, 316, and 319 in the former and Asn251, Arg254, and Gln255 in the latter. The final conformation is further stabilized by the newly formed interaction between the N-terminal helix of the coiled coil (e.g., Thr2, Lys4, Arg9, and the main chains of Leu3) and Asp315, Asp352, and Gln378 in the central domain of β_E. The α subunits also have complementary electrostatic interactions, but they appear to be less important than those of the β subunits because of the small motions involved.

Discussion

The molecular dynamics simulation of the 120° rotation step, which is the basic element in the functional cycle of F_1-ATPase, provides new insights concerning its mechanism. The central stalk made up of the γ, δ, and ϵ subunits rotates by 120°; the spherical domain composed of the interleaved α and β subunits does not

rotate during the simulation, but two of the β subunits undergo major conformational changes. The 120° rotation of the γ subunit in the direction of ATP synthesis results in the subunit structural "interchanges" $\beta_{TP} \rightarrow \beta_E$, $\beta_E \rightarrow \beta_{DP}$, and $\beta_{DP} \rightarrow \beta_{TP}$, with corresponding interchanges in the α subunits. The N-terminal domains and top part of the central domains of the α and β subunits are in contact and act to stabilize the assembly, but there is relatively little motion in this part of the molecule during the transition, in accord with the 6-fold pseudosymmetry observed in the X-ray structures. The β subunits undergo small but significant displacements (quaternary structural changes) in addition to the more important internal structural alterations (tertiary structural changes), e.g., the β_{TP} subunit moves downward and rotates outward in response to the rotation of the γ subunit. It is evident from a normal mode analysis, as is the case in GroEL [19], that the subunits are constructed such that the observed changes correspond to low-frequency modes (Q.C. et al., unpublished data).

The rotation of the γ subunit, engendered by the proton flux through F_o (the intrinsic membrane domain of the F_1F_o-ATP synthase complex) drives the conformational changes in the F_1 portion. The γ protrusion is shown by the molecular dynamics trajectory to be a key element in the mechanism and makes two highly important contributions to the conformational transition. The first is that its rotation induces that of the two-helix coiled coil making up the stalk of the γ subunit in the center of the $\alpha_3\beta_3$ assembly. The interactions of the coiled coil with the β subunits, primarily the hth motif in the C-terminal domain and a loop in the central domain, play an essential role in driving the conformation change. A second aspect is that the large number of positively charged Lys and Arg side chains on the γ protrusion form an ionic track, which acts to guide the conformational changes of the C-terminal domains of the β subunits, particularly their hth motifs.

It is interesting to speculate whether the ionic track plays an equally important role for other F_1-ATPases whose sequences are known but for which no structures are available. The alignment of 31 sequences, which is approximate because the sequence conservation of the γ subunit is low between residues 50–200, shows that six of the Lys and Arg in Figure 5 are highly conserved (in 23 or more out of the 31 sequences); they are Lys 30, Arg 33, Arg 42, Arg 75, Lys 87, and Arg 228. Most of the other residues show a conservation of about 30%. In the mitochondrial case studied here, the ionic track interactions during the rotation involved at least one highly conserved residue and some less well-conserved residues in each of the regions (see Figure 5). This suggests that not all charged residues are essential for forming a functional ionic track. However, since bacterial γ subunits can have only a very small number of ionic side chains in the track region, an alternative mechanism may be operative. A full analysis will have to wait until structural information becomes available.

The trajectory provides a detailed picture of the dynamics of the transition during the basic 120° cycle. The rotation of the helices in the coiled coil lags slightly behind that of the γ protrusion, due to the intrinsic flexibility of the former (as deduced from a normal mode analysis) and the force required to produce the conformational changes in the β subunits. The interactions involved are a combination of steric repulsions and electrostatic attractions. The β_E subunit is initially in the open conformation in contact with the γ bulge and moves inward into the γ groove as soon as the γ bulge has passed. This motion occurs essentially without a time lag during the BMD simulation, which applies a force only on the γ subunit. The motion of the β_E subunit involves interactions with the bound ADP ligand and the attractive interactions between the positive side chains of the γ subunit and the negative side chains of the hth motif; main chain carbonyls of the latter also play a role. The attraction between positive side chains in the middle of the γ coiled coil and an upper negatively charged loop of β_E contribute to the closing of the binding site, which is initiated by the motion of the hth motif. The final position of β_E is slightly stabilized by the newly formed β_E, β_{DP} attractive van der Waals contact. The outward motion of β_{TP}, which is originally in the γ groove, is initiated by repulsive interactions when the γ bend of the C-terminal helix collides with the hth motif. This is reinforced by the γ bulge of the N-terminal helix, which comes in contact with the hth motif of β_{TP} somewhat later in the trajectory. Throughout the conformational transition, the C-terminal subunit of β_{TP} is guided by its interactions with the ionic track of the γ protrusion. β_{DP} moves very little during the transition; it remains in the γ groove and exchanges its initial van der Waals contact with β_{TP} with an equivalent contact to β_E, which has replaced β_{TP} in the γ groove. The α subunits undergo only small distortions during the transition because their hth motifs are positioned further from the γ subunit.

F_1-ATPase emerges from the analysis based on the molecular dynamics trajectory as a finely tuned machine with steric repulsions and electrostatic attractions designed to yield the conformational changes required for its function. The simulation has elucidated the sequence of events that occur and the nature of the interactions involved. The rotation of the γ protrusion proceeds smoothly and steadily in the simulation. Overall, the large conformational changes of the β_{TP} and β_E subunits are approximately simultaneous. It has been suggested that the rotation is likely to have a significant "stochastic" element when it is driven by the proton-motive force engendered by the F_o complex and that a "thermal ratchet" mechanism is involved [20]. This would result in the response of the F_1-ATPase complex having a more diffusive character than that found in the trajectory. If the motion of the γ subunit due to F_o is globally unidirectional, the subunits are expected to alter their conformations during ATP synthesis in essential accord with the sequence obtained in the trajectory.

The present simulation was performed in the direction of ATP synthesis. In this process, the driving force for the rotation of the γ subunit is provided by the F_o complex, and the response of the surrounding α and β subunits are determined by the motion of the γ subunit. It is likely that, in the direction of ATP hydrolysis, the overall behavior of the subunits would be similar (in reverse) but that the microscopic details of the conformational changes may not be identical, given that the driving forces in the two processes are different. Specifically,

in the ATP hydrolysis mode, the source of the conformational change in the β subunits, which induces the rotation of the γ subunit, is thought to be the release of ATP, which results in a two-step rotation (90° plus 30°) [16]; this is not apparent in the present trajectory. Examination of the behavior in the ATP hydrolysis mode and of the role of the conformational change in catalysis is left for subsequent studies. An analysis will be made of the changes in ligand binding during the transition. Of interest in this regard is the recently determined "intermediate" structure with ligands in all three catalytic sites [11].

Biological Implications

F_1F_o-ATP synthase, found in eubacteria, chloroplasts, and mitochondria, is responsible for most of the ATP synthesis in living systems. An understanding of the function of this large multisubunit molecular machine is essential for knowing how ATP, the major energy currency of life, is synthesized in the cell. F_1F_o-ATP synthase functions as a 2-fold rotary motor in ATP synthesis. The membrane-bound (F_o) portion rotates due to a transmembrane proton-motive force generated by photosynthesis or respiration. The rotation of F_o induces a rotation of the central γ subunit of the F_1-ATPase, the globular structure outside the membrane. The molecular dynamics simulation of F_1-ATPase reported here demonstrates how the rotation of the γ subunit induces the opening and closing motions of the catalytic β subunits. The motions control the synthesis and release of newly formed ATP. The resulting trajectory provides a detailed view of the dynamics of the rotation. Of particular interest is the demonstration that there exists an ionic track that guides the motion of the β subunits during the rotational transition. The calculations provide a structural and energetic basis for the different positions (open and closed) of the β subunits in the X-ray structure during the rotation cycle. The molecular dynamics simulations reported here represent a first step in a unified description of F_1-ATPase. Future work will focus on the details of ATP synthesis and the release of ATP as a result of the subunit conformational change.

Experimental Procedures

The targeted molecular dynamics method [13], implemented in the CHARMM program [21], was employed to simulate the conformational transition of the F_1-ATPase. The approach is similar to that used in a corresponding study of the molecular chaperonin GroEL [22], another ATP-driven molecular motor complex [23].

This method uses a standard molecular mechanics potential energy function with solvent screening together with a time-dependent force, which is determined at each time step by the difference between the conformation of the moving structure and the target structure [13, 22]. The F_1-ATPase complex used in the simulations consisted of three α, three β, one γ, one δ and one ε subunit. It was constructed using two published crystal structures. The coordinates of the three α and the three β subunits were taken from the F_1-ATPase of bovine heart mitochondria [4] (Protein Data Bank code 1BMF), and the coordinates of the γ, δ, and ε subunits were taken from Gibbons et al. [15] (Protein Data Bank code 1E79). The full complex was constructed by superimposing the central coiled-coil portion of the γ subunit resolved in both crystal structures; the RMS difference between the two is 0.8 Å for the main chain. All three α subunits were modeled with ATP bound, and the three β subunits were modeled as follows: β_{DP} had an ATP molecule bound, β_{TP} was empty, and β_E had an ADP molecule bound; the nucleotides in the catalytic sites of the β subunits mimic those expected at the end of the 120° rotation step in the synthesis direction to facilitate the transition. The target conformation was obtained by first introducing an intermediate structure in which the labels correspond to the identities of the three α and three β subunits after the 120° rotation (i.e., $\alpha_E \leftarrow \alpha_{DP}$, $\alpha_{DP} \leftarrow \alpha_{TP}$, $\alpha_{TP} \leftarrow \alpha_E$, $\beta_E \leftarrow \beta_{DP}$, $\beta_{DP} \leftarrow \beta_{TP}$, and $\beta_{TP} \leftarrow \beta_E$). Given this subunit identification, the entire complex in the intermediate structure was superposed on the initial conformation based on a backbone least-square fit of the three α subunits. This assumes that the three α subunits do not undergo significant conformational changes during a complete ATP synthesis step, which is consistent with the X-ray structure. The resulting structure has the γ, δ, and ε subunits rotated by 120° and the three α and three β subunits in nearly the same physical position, but with altered conformations. No constraints were imposed during the simulation other than the standard TMD constraint connecting the two end structures [13], i.e., no portions of molecule were artificially anchored in space, and the TMD force was applied to the entire $\alpha_3\beta_3\gamma\delta\epsilon$ complex, but the water molecules and all ligands, including the Mg^{2+} ions, were free to move without any constraints.

The CHARMM all-atom protein potential energy function [24] was used to calculate the TMD trajectory. The length of all the bonds that involve hydrogen atoms were kept constant by the SHAKE algorithm [25]. A modified TIP3P potential [26, 27] was used for water molecules. A total of 603 water molecules taken from the waters in the X-ray structure (1BMF) were kept, and the nucleotides, both ATP and ADP, have their corresponding Mg^{2+} ions included.

Limiting the number of water molecules in the system, relative to full solvation, is a significant approximation but decreases the required computer time by more than two orders of magnitude, an important element in making multiple simulations for such large systems [22]. It has been shown that the physical properties of the system can be preserved by screening the charged groups and introducing a distance-dependent dielectric constant [28–30]. For the present analysis of the structural changes during the rotation cycles, a simple scaling of all the charged groups by a factor of 0.3 was used [29]. This model leads to a salt bridge strength in the range from 1 to 3 kcal/mol, in accord with the results of molecular dynamics simulations with full account of aqueous solvation [31], as well as mutation experiments involving charged groups [32]. Such scaling is essential for the present problem because of the important role of salt bridges in the mechanism. The system was equilibrated for 50 ps, prior to initiating the TMD trajectory. A time step of 2 fs was used for the dynamics with the leapfrog integration scheme [33], and the temperature was 300 K. Coordinates were saved every 0.4 ps. The initial rms difference between two structures was 10.7 Å, and the TMD trajectory was completed in 500 ps. This resulted in a trajectory consisting of 1250 coordinate sets, which were used for analysis. The observed motions during the transition are smooth, suggesting that there are no high barriers whose presence leads to distortion of the trajectory due to its short timescale. Moreover, comparison with the other TMD simulation, in which the transition occurred during 250 ps, and the BMD simulation, which is 1 ns in length (see below), showed very similar results (with the exception of the β_{TP} subunit behavior; see text), indicating that the simulation time is sufficiently long for a meaningful analysis. However, we cannot exclude that some of the distortions observed in the coiled coil (see above) are a consequence of the short timescale, though they are likely to be real, given the interactions involved. Results on the use of similar short time simulations for the conformational change in GroEL [22] have been confirmed by experiment [34–36], as they have for protein unfolding simulations on a corresponding timescale [37].

In addition to the TMD simulation, a biased molecular dynamics simulation (BMD) [14] of 1 ns with a 1 fs time step was performed with the CHARMM program [21]. In the trajectory, the bias was applied only to the γ subunit, and the α and β subunits were allowed to respond without constraints. Normal mode calculations were made following standard methods with the VIBRAN module in the CHARMM program [21, 38]. Results from these simulations are included where appropriate. The TMD simulation of 500 ps for the 120° rotation cycle required about 240 cpu hours on a single-processor SGI Indigo.

Acknowledgments

We thank Y. Kong, K. Huang, and W. Yang for aid with the figures. M.K. thanks the National Institutes of Health and J.P.M. thanks the Welsh Foundation for partial support of this research. Figures were made with the programs MolScript [39] and QUANTA from Accelrys. Some of the calculations were done on the Origin 2000 at the National Cancer Institute.

Received: November 29, 2001
Revised: March 11, 2002
Accepted: April 23, 2002

References

1. Weber, J., and Senior, A.E. (1997). Catalytic mechanism of F_1-ATPase. Biochim. Biophys. Acta *1319*, 19–58.
2. Boyer, P.D. (1998). Energy, life and ATP (Nobel Lecture). Angew. Chem. Int. Ed. Engl. *37*, 2296–2307.
3. Walker, J.E. (1998). ATP synthesis by rotary catalysis (Nobel Lecture). Angew. Chem. Int. Ed. Engl. *37*, 2309–2319.
4. Abrahams, J.P., Leslie, A.G.W., Lutter, R., and Walker, J.E. (1994). Structure at 2.8 Å resolution of F_1-ATPase from bovine heart mitochondria. Nature *370*, 621–628.
5. Stock, D., Leslie, A.G.W., and Walker, J.E. (1999). Molecular architecture of the rotary motor in ATP synthase. Science *286*, 1700–1705.
6. Seelert, H., Poetsch, A., Dencher, N.A., Engel, A., Stahlberg, H., and Muller, D.J. (2000). Structural biology—proton-powered turbine of a plant motor. Nature *405*, 418–419.
7. Jiang, W., Hermoalin, J., and Fillingame, R.H. (2001). The preferred stoichiometry of the c subunits in the rotary motor of Escherichia coli ATP synthase is 10. Proc. Natl. Acad. Sci. USA *98*, 4966–4971.
8. Stahlberg, H., Muller, D.J., Suda, K., Fotiadis, D., Engel, A., Meier, T., Matthey, U., and Dimroth, P. (2001). Bacterial Na^+-ATP synthase has an undecameric rotor. EMBO Rep. *2*, 229–233.
9. Boyer, P.D. (1993). The binding change mechanism for ATP synthase, some probabilities and possibilities. Biochim. Biophys. Acta *1140*, 215–250.
10. Boyer, P.D. (1997). The ATP synthase—a splendid molecular machine. Annu. Rev. Biochem. *66*, 717–749.
11. Menz, R.I., Walker, J.E., and Leslie, A.G.W. (2001). Structure of bovine mitochondrial F_1-ATPase with nucleotide bound to all three catalytic sites: implications for the mechanism of rotary catalysis. Cell *106*, 331–341.
12. Noji, H., Yasuda, R., Yoshida, M., and Kinoshita, K., Jr. (1997). Direct observation of the rotation of F_1-ATPase. Nature *386*, 299–302.
13. Schlitter, J., Engels, M., Kruger, P., Jacoby, E., and Wollmer, A. (1993). Targeted molecular dynamics simulation of conformational change—application to the T-R transition in insulin. Mol. Simul. *10*, 291–308.
14. Paci, E., and Karplus, M. (1999). Forced unfolding of fibronectin type 3 modules: an analysis by biased molecular dynamics simulations. J. Mol. Biol. *288*, 441–459.
15. Gibbons, C., Montgomery, M.G., Leslie, A.G.W., and Walker, J.E. (2000). The structure of the central stalk in bovine F(1)-ATPase at 2.4 Å resolution. Nat. Struct. Biol. *7*, 1055–1061.
16. Yasuda, R., Noji, H., Yoshida, M., Kinosita, K., Jr., and Itoh, H. (2001). Resolution of distinct rotational substeps by submillisecond kinetic analysis of F1-ATPase. Nature *410*, 898–904.
17. Masaike, T., Mitome, N., Noji, H., Muneyuki, E., Yasuda, R., Kinosita, K., Jr., and Yoshida, M. (2000). Rotation of F_1-ATPase and the hinge residues of the β subunit. J. Exp. Biol. *203*, 1–8.
18. Hara, K.Y., Noji, H., Bald, D., Yasuda, R., Kinosita, K., Jr., and Yoshida, M. (2000). The role of the DELSEED motif of the β subunit in rotation of F_1-ATPase. J. Biol. Chem. *275*, 14260–14263.
19. Ma, J., and Karplus, M. (1998). The allosteric mechanism of the chaperonin GroEL: a dynamic analysis. Proc. Natl. Acad. Sci. USA *95*, 8502–8507.
20. Bustamante, C., Keller, D., and Oster, G. (2001). The physics of molecular motors. Acc. Chem. Res. *34*, 412–420.
21. Brooks, B.R., Bruccoleri, R.E., Olafson, B.D., States, D.J., Swaminathan, S., and Karplus, M. (1983). CHARMM: a program for macromolecular energy, minimization, and dynamics calculations. J. Comput. Chem. *4*, 187–217.
22. Ma, J., Sigler, P.B., Xu, Z., and Karplus, M. (2000). A dynamic model for the allosteric mechanism of GroEL. J. Mol. Biol. *302*, 303–313.
23. Sigler, P.B., Xu, Z., Rye, H.S., Burston, S.G., Fenton, W.A., and Horwich, A.L. (1998). Structure and function in GroEL-mediated protein folding. Annu. Rev. Biochem. *67*, 581–608.
24. MacKerell, A.D., Jr., Bashford, D., Bellott, M., Dunbrack, R.L., Jr., Evanseck, J.D., Field, M.J., Fischer, S., Gao, J., Guo, H., Ha, S., et al. (1998). All-atom empirical potential for molecular modeling and dynamics studies of proteins. J. Phys. Chem. B *102*, 3586–3616.
25. Ryckaert, J.P., Ciccotti, G., and Berendsen, H.J.C. (1977). Numerical integration of the Cartesian equations of motion of a system with constraints: molecular dynamics of n-alkanes. J. Comput. Phys. *23*, 327–341.
26. Jorgensen, W.L. (1981). Transferable intermolecular potential functions for water, alcohols, and ethers. Application to liquid water. J. Am. Chem. Soc. *103*, 335–340.
27. Neria, E., Fischer, S., and Karplus, M. (1996). Simulation of activation free energies in molecular systems. J. Chem. Phys. *105*, 1902–1921.
28. Brooks, C.L., III, Karplus, M., and Pettitt, B.M. (1988). Proteins: a theoretical perspective of dynamics, structure, and thermodynamics. Adv. Chem. Phys. *71*, 1–249.
29. Northrup, S.H., Pear, M.R., McCammon, J.A., and Karplus, M. (1980). Molecular dynamics of ferrocytochrome c. Nature *286*, 304–305.
30. Fischer, S., Michnick, S., and Karplus, M. (1994). A mechanism for rotamase catalysis by the FK506 binding protein (FKBP). Biochemistry *32*, 13830–13837.
31. Simonson, T., Archontis, G., and Karplus, M. (1997). Continuum treatment of long-range interactions in free energy calculations. Application to protein-ligand binding. J. Phys. Chem. *41*, 8347–8360.
32. Fersht, A. (1998). Enzyme Structure, Mechanism and Protein Folding, Third Edition (New York: W. H. Freeman).
33. Allen, M.P., and Tildesley, D.J. (1980). Computer Simulation of Liquids (Oxford: Clarendon Press).
34. Thirumalai, D., and Lorimer, G.H. (2001). Chaperonin-mediated protein folding. Annu. Rev. Biophys. Biomol. Struct. *30*, 245–269.
35. Shiseki, K., Murai, N., Motojima, F., Hisabori, T., Yoshida, M., and Taguchi, H. (2001). Synchronized domain-opening motion of GroEL is essential for communcation between the two rings. J. Biol. Chem. *276*, 11335–11338.
36. Ranson, N.A., Farr, G.W., Roseman, A.M., Gowen, B., Fenton, W.A., Horwich, A.L., and Saibil, H.R. (2001). ATP bound state captured by cryo-electron microscopy. Cell *107*, 869–879.
37. Marszalek, P.E., Lu, H., Li, H., Carrion-Vazquez, M., Oberhauser, A.F., Schulten, K., and Fernandez, J.M. (1999). Mechanical unfolding intermediates in titin modules. Nature *402*, 100–103.
38. Brooks, B.R., Janeic, D., and Karplus, M. (1995). Harmonic analysis of large systems. I. Methodology. J. Comp. Chem. *1616*, 1522–1542.
39. Kraulis, P.J. (1991). MolScript: a program to produce both detailed and schematic plots of protein structures. J. Appl. Crystallogr. *24*, 946–950.